**Steel and Composite Structures**, *Vol. 22, No. 2 (2016) 257-276*
DOI: http://dx.doi.org/10.12989/scs.2016.22.2.257


# A new simple three-unknown sinusoidal shear deformation theory for functionally graded plates

Mohammed Sid Ahmed Houari [1,2], Abdelouahed Tounsi [*2,3], Aicha Bessaim [1,2] and S.R. Mahmoud [4,5]

[1] *Université Mustapha Stambouli de Mascara, Department of Civil Engineering, Mascara, Algeria*
[2] *Material and Hydrology Laboratory, University of Sidi Bel Abbes, Faculty of Technology, Civil Engineering Department, Algeria*
[3] *Laboratoire de Modélisation et Simulation Multi-échelle, Département de Physique, Faculté des Sciences Exactes, Département de Physique, Université de Sidi Bel Abbés, Algeria*
[4] *Department of Mathematics, Faculty of Science, King Abdulaziz University, Saudi Arabia*
[5] *Mathematics Department, Faculty of Science, University of Sohag, Egypt*

(*Received July 10, 2016, Revised September 25, 2016, Accepted September 30, 2016*)

**Abstract.** In this paper, a new simple higher-order shear deformation theory for bending and free vibration analysis of functionally graded (FG) plates is developed. The significant feature of this formulation is that, in addition to including a sinusoidal variation of transverse shear strains through the thickness of the plate, it deals with only three unknowns as the classical plate theory (CPT), instead of five as in the well-known first shear deformation theory (FSDT) and higher-order shear deformation theory (HSDT). A shear correction factor is, therefore, not required. Equations of motion are derived from Hamilton's principle. Analytical solutions for the bending and free vibration analysis are obtained for simply supported plates. The accuracy of the present solutions is verified by comparing the obtained results with those predicted by classical theory, first-order shear deformation theory, and higher-order shear deformation theory. Verification studies show that the proposed theory is not only accurate and simple in solving the bending and free vibration behaviours of FG plates, but also comparable with the other higher-order shear deformation theories which contain more number of unknowns.

**Keywords:** a simple 3-unknown theory; bending; vibration; functionally graded plates

## 1. Introduction

Nowadays functionally graded materials (FGMs) are an alternative materials widely used in aerospace, nuclear, civil, automotive, optical, biomechanical, electronic, chemical, mechanical and shipbuilding industries. In fact, FGMs have been proposed, developed and successfully used in industrial applications since 1980's (Koizumi 1993). The increase of FGM applications requires the development of accurate theories to predict their responses (Kar and Panda 2015a, Akbaş 2015, Darılmaz 2015, Ait Atmane *et al*. 2015, Al-Basyouni *et al*. 2015, Arefi *et al*. 2015, Bennai *et al*. 2015, Meradjah *et al*. 2015). Many studies have been developed for thermal stress, hygro-thermo-elastic bending, thermal and mechanical buckling, and linear and nonlinear free vibration of

*Corresponding author, Ph.D., E-mail: houarimsa@yahoo.fr


http://www.techno-press.org/?journal=scs&subpage=6 ISSN: 1229-9367 (Print), 1598-6233 (Online)

laminated composite and multilayered structures are available in the literature (Tounsi *et al*. 2013, Belabed *et al*. 2014, Zidi *et al*. 2014, Bouchafa *et al*. 2015, Larbi Chaht *et al*. 2015, Belkorissat *et al*. 2015, Sahoo *et al*. 2016a, 2016b, Mahapatra *et al*. 2016a, b, c, Bousahla *et al*. 2016). Draiche *et al*. (2014) examined the free vibration of rectangular composite plates with patch mass by employing a trigonometric four variable plate model. Bousahla *et al*. (2014) developed a novel higher order shear and normal deformation theory based on neutral surface position for bending analysis of advanced composite plates. Khalfi *et al*. (2014) used a refined and simple shear deformation theory for thermal buckling of solar functionally graded plates resting on elastic foundation. Kar and Panda (2015b) studied the free vibration responses of shear deformable functionally graded curved panels under uniform, linear and nonlinear temperature fields based on the higher-order shear deformation. Ait Yahia *et al*. (2015) studied the wave propagation in FG plates with porosities using various higher-order shear deformation plate theories. Beldjelili *et al*. (2016) investigated the hygro-thermo-mechanical bending of S-FGM plates resting on variable elastic foundations using a four-variable trigonometric plate theory. Bounouara *et al*. (2016) presented a nonlocal zeroth-order shear deformation theory for free vibration of FG nanoscale plates resting on elastic foundation. It should be noted that the classical plate theory (CPT), which is based on the Kirchhoff hypothesis, is suitable for thin plates, but inadequate for thick plates or plates made of advanced composites like FGMs. The first order shear deformation theory (FSDT) (Bellifa *et al*. 2016, Yaghoobi and Yaghoobi 2013, Zhao *et al*. 2009) accounts for the shear deformation effect by the way of linear variation of in-plane displacements through the thickness. Thus, a shear correction factor is required to compensate for the difference between the actual and assumed constant stress states. The higher-order shear deformation theories (Reddy 1984, 2000, Ren 1986, Kant and Pandya 1988, Pandya and Kant 1988, Touratier 1991, Zenkour 2006, Soldatos 1992, Karama *et al*. 2003, Pradyumna and Bandyopadhyay 2008, Jha *et al*. 2013, Bachir Bouiadjra *et al*. 2013, Bouderba *et al*. 2013, Tounsi *et al*. 2013, Ait Amar Meziane *et al*. 2014, Attia *et al*. 2014, Hamidi *et al*. 2015, Mahi *et al*. 2015, Bourada *et al*. 2015, Akavci 2015, Mantari *et al*. 2016, Amirpour *et al*. 2016, Bennoun *et al*. 2016, Bouderba *et al*. 2016) account for higher-order variation in the in-plane displacements through the thickness of the plate and satisfy the equilibrium conditions at the top and bottom surfaces of the plate and, consequently, any shear correction factors are needed. These theories are capable of representing the section warping in the deformed configuration. The major advantage of this theories is that the transverse shear strains and stresses are represented quadratically, a state of tress that is close to the 3-D elasticity solution they have the ability to change the transverse strain and stress distribution (Aydogdu 2006). Some of these higher-order shear deformation theories are cumbersome and computationally expensive since with each additional power of the thickness coordinate, an additional unknown is introduced to the theory (e.g., theories by Ren (1986) with nine unknowns, Kant and Pandya (1988) with seven unknowns, Pandya and Kant (1988) with nine unknowns, Pradyumna and Bandyopadhyay (2008) with nine unknowns, Jha *et al*. (2013) with twelve unknowns and recently, Tounsi *et al*. (2013), Boukhari *et al*. (2016) and Bourada *et al*. (2016) with four unknowns. Although some well-known higher-order shear deformation theories have the same unknowns as in the first-order shear deformation theory (e.g., third-order shear deformation theory (Reddy 1984, 2000), sinusoidal shear deformation theory (Touratier 1991, Zenkour 2006), hyperbolic shear deformation theory (Soldatos 1992), and exponential shear deformation theory (Karama *et al*. 2003), their equations of motion are more complicated than those of the first-order shear deformation theory. As a consequence, the development of simple higher-order shear deformation theories in the present work is necessary.

This work aims to develop a new simple higher-order shear deformation theory for the bending and vibration analyses of FG plates. The proposed theory contain fewer unknowns and equations of motion than the first-order shear deformation theory, but satisfy the equilibrium conditions at the top and bottom surfaces of the plate without using any shear correction factors. Indeed, unlike the previous mentioned theories, the number of variables in the present theory is same as that in the CPT. Equations of motion are derived from Hamilton's principle. Analytical solutions for deflections, stresses, and frequencies are obtained for a simply supported FG plate. Numerical examples are presented to verify the accuracy of the present theory.

## 2. Theoretical formulation

Consider a simply supported rectangular FG plate with the length $a$, width $b$, and thickness $h$. The $x$-, $y$-, and $z$-coordinates are taken along the length, width, and height of the plate, respectively, as shown in Fig. 1. The formulation is limited to linear elastic material behavior. The FG plate is isotropic with its material properties vary smoothly through the thickness of the plate. Unlike the previous mentioned theories, the number of unknown functions involved in the present theory is only three as in CPT.

### *2.1 Kinematics*

The displacement field of the present three unknowns shear deformation theory is built upon the classical plate theory (CPT) including the sinusoidal function in terms of thickness coordinate to represent shear deformation and is assumed as follows (Tounsi *et al*. 2016)

$$\begin{aligned} u(x,y,z,t) &= u_0(x,y,t) - z\frac{\partial w_0}{\partial x} - f(z)\frac{\partial^3 w_0}{\partial x^3} \\ v(x,y,z,t) &= v_0(x,y,t) - z\frac{\partial w_0}{\partial y} - f(z)\frac{\partial^3 w_0}{\partial y^3} \\ w(x,y,z,t) &= w_0(x,y,t) \end{aligned} \tag{1}$$

where $u_0$, $v_0$, and $w_0$ are three unknown displacement functions of midplane of the plate. $f(z)$ is a shape function representing the distribution of the transverse shear strains and shear stresses

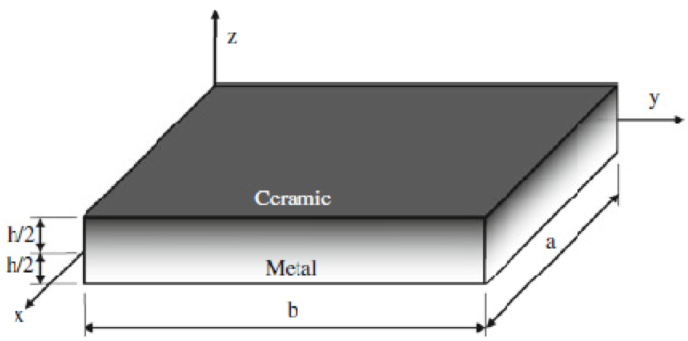


Fig. 1 Geometry of rectangular FG plate and coordinates

through the thickness of the plate and is given as

$$f(z) = \cosh\left(\frac{\pi}{2}\right)\frac{h^3}{2\pi^2}\sin\left(\frac{\pi z}{h}\right), \tag{2}$$

The nonzero strains associated with the displacement field in Eq. (1) are

$$\begin{Bmatrix} \varepsilon_x \\ \varepsilon_y \\ \gamma_{xy} \end{Bmatrix} = \begin{Bmatrix} \varepsilon_x^0 \\ \varepsilon_y^0 \\ \gamma_{xy}^0 \end{Bmatrix} + z\begin{Bmatrix} k_x \\ k_y \\ k_{xy} \end{Bmatrix} + f(z)\begin{Bmatrix} \eta_x \\ \eta_y \\ \eta_{xy} \end{Bmatrix}, \qquad \begin{Bmatrix} \gamma_{yz} \\ \gamma_{xz} \end{Bmatrix} = g(z)\begin{Bmatrix} \gamma_{yz}^0 \\ \gamma_{xz}^0 \end{Bmatrix}, \tag{3}$$

where

$$\begin{Bmatrix} \varepsilon_x^0 \\ \varepsilon_y^0 \\ \gamma_{xy}^0 \end{Bmatrix} = \begin{Bmatrix} \dfrac{\partial u_0}{\partial x} \\ \dfrac{\partial v_0}{\partial x} \\ \dfrac{\partial u_0}{\partial y} + \dfrac{\partial v_0}{\partial x} \end{Bmatrix}, \quad \begin{Bmatrix} k_x \\ k_y \\ k_{xy} \end{Bmatrix} = \begin{Bmatrix} -\dfrac{\partial^2 w_0}{\partial x^2} \\ -\dfrac{\partial^2 w_0}{\partial y^2} \\ -2\dfrac{\partial^2 w_0}{\partial x \partial y} \end{Bmatrix}, \quad \begin{Bmatrix} \eta_x \\ \eta_y \\ \eta_{xy} \end{Bmatrix} = \begin{Bmatrix} -\dfrac{\partial^4 w_0}{\partial x^2} \\ -\dfrac{\partial^4 w_0}{\partial y^2} \\ -\dfrac{\partial^2 (\nabla^2 w_0)}{\partial x \partial y} \end{Bmatrix}, \quad \begin{Bmatrix} \gamma_{yz}^0 \\ \gamma_{xz}^0 \end{Bmatrix} = \begin{Bmatrix} -\dfrac{\partial^3 w_0}{\partial y^3} \\ -\dfrac{\partial^3 w_0}{\partial x^3} \end{Bmatrix}, \tag{4}$$

and

$$g(z) = f'(z), \quad \nabla^2 w_0 = \frac{\partial^2 w_0}{\partial x^2} + \frac{\partial^2 w_0}{\partial y^2} \tag{5}$$

### *2.2 Constitutive relations*

The material properties of FG plates are assumed to vary continuously through the thickness. Three homogenization methods are deployable for the computation of the Young's modulus $E(z)$ namely: (1) the power law distribution; and (2) the Mori-Tanaka scheme. For the power law distribution, the Young's modulus is given as (Reddy 2000)

$$E(z) = E_m + (E_c - E_m)\left(\frac{2z + h}{2h}\right)^k \tag{6}$$

where $k$ is the power law index; and the subscripts $m$ and $c$ represent the metallic and ceramic constituents, respectively.

For Mori-Tanaka scheme, the Young's modulus is given as (Benveniste 1987, Mori and Tanaka 1973)

$$E(z) = E_m + (E_c - E_m)\left(\frac{V_c}{1 + (1 - V_c)(E_c / E_m - 1)(1 + \nu)/(3 - 3\nu)}\right) \tag{7}$$

where $V_c = (0.5 + z/h)^k$ is the volume fraction of the ceramic. Since the effects of the variation of Poisson's ratio ($\nu$) on the response of FGM plates are very small (Yang *et al*. 2005, Kitipornchai *et* *al*. 2006), this material parameter is assumed to be constant for convenience. The linear constitutive relations of a FG plate can be written as

$$\begin{Bmatrix} \sigma_x \\ \sigma_y \\ \tau_{yz} \\ \tau_{xz} \\ \tau_{xy} \end{Bmatrix} = \begin{bmatrix} C_{11} & C_{12} & 0 & 0 & 0 \\ C_{12} & C_{22} & 0 & 0 & 0 \\ 0 & 0 & C_{44} & 0 & 0 \\ 0 & 0 & 0 & C_{55} & 0 \\ 0 & 0 & 0 & 0 & C_{66} \end{bmatrix} \begin{Bmatrix} \varepsilon_x \\ \varepsilon_y \\ \gamma_{yz} \\ \gamma_{xz} \\ \gamma_{xy} \end{Bmatrix} \tag{8}$$

where ($\sigma_x$, $\sigma_y$, $\tau_{yz}$, $\tau_{xz}$, $\tau_{xy}$) and ($\varepsilon_x$, $\varepsilon_y$, $\gamma_{yz}$, $\gamma_{xz}$, $\gamma_{xy}$) are the stress and strain components, respectively. The stiffness coefficients, $C_{ij}$, can be expressed as

$$C_{11} = C_{22} = \frac{E(z)}{1-\nu^2}, \qquad C_{12} = \nu\, C_{11} \tag{9a}$$

$$C_{44} = C_{55} = C_{66} = G(z) = \frac{E(z)}{2(1+\nu)}, \tag{9b}$$

### 2.3 Equations of motion

Hamilton’s principle is used herein to derive equations of motion. The principle can be stated in an analytical form as follows

$$0 = \int_0^T (\delta U + \delta V - \delta K) dt \tag{10}$$

where $\delta U$ is the variation of strain energy; $\delta V$ is the variation of work done by external forces; and $\delta K$ is the variation of kinetic energy.

The variation of strain energy of the plate is calculated by

$$\begin{aligned} \delta U &= \int_{-h/2}^{h/2} \int_A \left[ \sigma_x \delta\, \varepsilon_x + \sigma_y \delta\, \varepsilon_y + \tau_{xy} \delta\, \gamma_{xy} + \tau_{yz} \delta\, \gamma_{yz} + \tau_{xz} \delta\, \gamma_{xz} \right] dA\, dz \\ &= \int_A \left[ N_x \delta\, \varepsilon_x^0 + N_y \delta\, \varepsilon_y^0 + N_{xy} \delta\, \gamma_{xy}^0 + M_x \delta\, k_x + M_y \delta\, k_y + M_{xy} \delta\, k_{xy} \right. \\ &\quad \left. + S_x \delta\, \eta_x + S_y \delta\, \eta_y + S_{xy} \delta\, \eta_{xy} + Q_{yz} \delta\, \gamma_{yz}^0 + Q_{xz} \delta\, \gamma_{xz}^0 \right] dA = 0 \end{aligned} \tag{11}$$

where $A$ is the top surface and the stress resultants $N$, $M$, $S$ and $Q$ are defined by

$$(N_i, M_i, S_i) = \int_{-h/2}^{h/2} (1, z, f) \sigma_i dz, \quad (i = x, y, xy) \quad \text{and} \quad Q_i = \int_{-h/2}^{h/2} \tau_i g(z) dz, \quad (i = xz, yz) \tag{12}$$

The variation of work done by external forces can be expressed as

$$\delta V = -\int_A q \delta\, w_0 dA \tag{13}$$

where $q$ is the distributed transverse load.

The variation of kinetic energy of the plate can be written in the form

$$\begin{aligned}\delta K &= \int_{-h/2}^{h/2} \int_A \left[\dot{u}\delta\,\dot{u} + \dot{v}\delta\,\dot{v} + \dot{w}\delta\,\dot{w}\right]\rho(z)\,dA\,dz \\ &= \int_A \Big\{ I_0\left[\dot{u}_0\delta\dot{u}_0 + \dot{v}_0\delta\dot{v}_0 + \dot{w}_0\delta\dot{w}_0\right] \\ &\quad - I_1\left(\dot{u}_0\frac{\partial\delta\dot{w}_0}{\partial x} + \frac{\partial\dot{w}_0}{\partial x}\delta\,\dot{u}_0 + \dot{v}_0\frac{\partial\delta\dot{w}_0}{\partial y} + \frac{\partial\dot{w}_0}{\partial y}\delta\,\dot{v}_0\right) \\ &\quad - J_1\left(\dot{u}_0\frac{\partial^3\delta\dot{w}_0}{\partial x^3} + \frac{\partial^3\dot{w}_0}{\partial x^3}\delta\,\dot{u}_0 + \dot{v}_0\frac{\partial^3\delta\dot{w}_0}{\partial y^3} + \frac{\partial^3\dot{w}_0}{\partial y^3}\delta\,\dot{v}_0\right) \\ &\quad + I_2\left(\frac{\partial\dot{w}_0}{\partial x}\frac{\partial\delta\,\dot{w}_0}{\partial x} + \frac{\partial\dot{w}_0}{\partial y}\frac{\partial\delta\,\dot{w}_0}{\partial y}\right) + K_2\left(\frac{\partial^3\dot{w}_0}{\partial x^3}\frac{\partial^3\delta\,\dot{w}_0}{\partial x^3} + \frac{\partial^3\dot{w}_0}{\partial y^3}\frac{\partial^3\delta\,\dot{w}_0}{\partial y^3}\right) \\ &\quad + J_2\left(\frac{\partial\dot{w}_0}{\partial x}\frac{\partial^3\delta\,\dot{w}_0}{\partial x^3} + \frac{\partial^3\dot{w}_0}{\partial x^3}\frac{\partial\delta\,\dot{w}_0}{\partial x} + \frac{\partial\dot{w}_0}{\partial y}\frac{\partial^3\delta\,\dot{w}_0}{\partial y^3} + \frac{\partial^3\dot{w}_0}{\partial y^3}\frac{\partial\delta\,\dot{w}_0}{\partial y}\right)\Big\} dA\end{aligned} \tag{14}$$

where dot-superscript convention indicates the differentiation with respect to the time variable $t$; $\rho(z)$ is the mass density; and $(I_0, I_1, J_1, I_2, J_2, K_2)$ are mass inertias defined as

$$\left(I_0, I_1, J_1, I_2, J_2, K_2\right) = \int_{-h/2}^{h/2}\left(1, z, f, z^2, z\,f, f^2\right)\rho(z)dz \tag{15}$$

Substituting the expressions for $\delta U$, $\delta V$, and $\delta K$ from Eqs. (11), (13), and (14) into Eq. (10) and integrating by parts, and collecting the coefficients of $\delta u_0$, $\delta v_0$ and $\delta w_0$, the following equations of motion of the plate are obtained

$$\begin{aligned}&\delta\,u_0:\ \frac{\partial N_x}{\partial x} + \frac{\partial N_{xy}}{\partial y} = I_0\ddot{u}_0 - I_1\frac{\partial\ddot{w}_0}{\partial x} - J_1\frac{\partial^3\ddot{w}_0}{\partial x^3} \\ &\delta\,v_0:\ \frac{\partial N_{xy}}{\partial x} + \frac{\partial N_y}{\partial y} = I_0\ddot{u}_0 - I_1\frac{\partial\ddot{w}_0}{\partial y} - J_1\frac{\partial^3\ddot{w}_0}{\partial y^3} \\ &\delta\,w_0:\ \frac{\partial^2 M_x}{\partial x^2} + 2\frac{\partial^2 M_{xy}}{\partial x\partial y} + \frac{\partial^2 M_y}{\partial y^2} + \frac{\partial^4 S_x}{\partial x^4} + \frac{\partial^4 S_{xy}}{\partial x^3\partial y} + \frac{\partial^4 S_{xy}}{\partial y^3\partial x} + \frac{\partial^4 S_y}{\partial y^4} \\ &\qquad - \frac{\partial^3 Q_{xz}}{\partial x^3} - \frac{\partial^3 Q_{yz}}{\partial y^3} + q = I_0\ddot{w}_0 + I_1\left(\frac{\partial\ddot{u}_0}{\partial x} + \frac{\partial\ddot{v}_0}{\partial y}\right) + J_1\left(\frac{\partial^3\ddot{u}_0}{\partial x^3} + \frac{\partial^3\ddot{v}_0}{\partial y^3}\right) - I_2\left(\frac{\partial^2\ddot{w}_0}{\partial x^2} + \frac{\partial^2\ddot{w}_0}{\partial y^2}\right)\end{aligned} \tag{16}$$

$$-2J_2\left(\frac{\partial^4 \ddot{w}_0}{\partial x^4}+\frac{\partial^4 \ddot{w}_0}{\partial y^4}\right)-K_2\left(\frac{\partial^6 \ddot{w}_0}{\partial x^6}+\frac{\partial^6 \ddot{w}_0}{\partial y^6}\right) \tag{16}$$

By substituting Eq. (3) into Eq. (8) and the subsequent results into Eq. (12), the stress resultants are obtained as

$$\begin{Bmatrix} N \\ M \\ S \end{Bmatrix}=\begin{bmatrix} A & B & B^s \\ B & D & D^s \\ B^s & D^s & H^s \end{bmatrix}\begin{Bmatrix} \varepsilon \\ k \\ \eta \end{Bmatrix}, \quad Q=A^s\gamma, \tag{17}$$

in which

$$N=\{N_x, N_y, N_{xy}\}^t, \quad M^b=\{M_x^b, M_y^b, M_{xy}^b\}^t, \quad S=\{S_x, S_y, S_{xy}\}^t, \tag{18a}$$

$$\varepsilon=\{\varepsilon_x^0, \varepsilon_y^0, \gamma_{xy}^0\}^t, \quad k=\{k_x, k_y, k_{xy}\}^t, \quad \eta=\{\eta_x, \eta_y, \eta_{xy}\}^t, \tag{18b}$$

$$A=\begin{bmatrix} A_{11} & A_{12} & 0 \\ A_{12} & A_{22} & 0 \\ 0 & 0 & A_{66} \end{bmatrix}, \quad B=\begin{bmatrix} B_{11} & B_{12} & 0 \\ B_{12} & B_{22} & 0 \\ 0 & 0 & B_{66} \end{bmatrix}, \quad D=\begin{bmatrix} D_{11} & D_{12} & 0 \\ D_{12} & D_{22} & 0 \\ 0 & 0 & D_{66} \end{bmatrix}, \tag{18c}$$

$$B^s=\begin{bmatrix} B_{11}^s & B_{12}^s & 0 \\ B_{12}^s & B_{22}^s & 0 \\ 0 & 0 & B_{66}^s \end{bmatrix}, \quad D^s=\begin{bmatrix} D_{11}^s & D_{12}^s & 0 \\ D_{12}^s & D_{22}^s & 0 \\ 0 & 0 & D_{66}^s \end{bmatrix}, \quad H^s=\begin{bmatrix} H_{11}^s & H_{12}^s & 0 \\ H_{12}^s & H_{22}^s & 0 \\ 0 & 0 & H_{66}^s \end{bmatrix}, \tag{18d}$$

$$Q=\{Q_{xz}, Q_{yz}\}^t, \quad \gamma=\{\gamma_{xz}^0, \gamma_{yz}^0\}^t, \quad A^s=\begin{bmatrix} A_{44}^s & 0 \\ 0 & A_{55}^s \end{bmatrix}, \tag{18e}$$

and stiffness components are given as

$$\begin{Bmatrix} A_{11} & B_{11} & D_{11} & B_{11}^s & D_{11}^s & H_{11}^s \\ A_{12} & B_{12} & D_{12} & B_{12}^s & D_{12}^s & H_{12}^s \\ A_{66} & B_{66} & D_{66} & B_{66}^s & D_{66}^s & H_{66}^s \end{Bmatrix}=\int_{-h/2}^{h/2} C_{11}\left(1, z, z^2, f(z), z\,f(z), f^2(z)\right)\begin{Bmatrix} 1 \\ \nu \\ \dfrac{1-\nu}{2} \end{Bmatrix} dz, \tag{19a}$$

$$\left(A_{22}, B_{22}, D_{22}, B_{22}^s, D_{22}^s, H_{22}^s\right)=\left(A_{11}, B_{11}, D_{11}, B_{11}^s, D_{11}^s, H_{11}^s\right), \tag{19b}$$

$$A_{44}^s=A_{55}^s=\int_{-h/2}^{h/2} C_{44}\left[g(z)\right]^2 dz, \tag{19c}$$

By substituting Eq. (17) into Eq. (16), the equations of motion can be expressed in terms of displacements ($u_0$, $v_0$ and $w_0$) as

$$
\begin{aligned}
& A_{11}\frac{\partial^2 u_0}{\partial x^2}+A_{66}\frac{\partial^2 u_0}{\partial y^2}+\left(A_{12}+A_{66}\right)\frac{\partial^2 v_0}{\partial x\partial y}-B_{11}\frac{\partial^3 w_0}{\partial x^3}-\left(B_{12}+2B_{66}\right)\frac{\partial^3 w_0}{\partial x\partial y^2} \\
& -B_{66}^s\frac{\partial^5 w_0}{\partial x^3\partial y^2}-\left(B_{12}^s+B_{66}^s\right)\frac{\partial^5 w_0}{\partial x\partial y^4}-B_{11}^s\frac{\partial^5 w_0}{\partial x^5}=I_0\ddot{u}_0-I_1\frac{\partial\ddot{w}_0}{\partial x}-J_1\frac{\partial^3\ddot{w}_0}{\partial x^3},
\end{aligned}
\tag{20a}
$$

$$
\begin{aligned}
& A_{22}\frac{\partial^2 v_0}{\partial y^2}+A_{66}\frac{\partial^2 v_0}{\partial x^2}+\left(A_{12}+A_{66}\right)\frac{\partial^2 u_0}{\partial x\partial y}-B_{22}\frac{\partial^3 w_0}{\partial y^3}-\left(B_{12}+2B_{66}\right)\frac{\partial^3 w_0}{\partial x^2\partial y} \\
& -B_{66}^s\frac{\partial^5 w_0}{\partial x^2\partial y^3}-\left(B_{12}^s+B_{66}^s\right)\frac{\partial^5 w_0}{\partial x^4\partial y}-B_{22}^s\frac{\partial^5 w_0}{\partial y^5}=I_0\ddot{v}_0-I_1\frac{\partial\ddot{w}_0}{\partial y}-J_1\frac{\partial^3\ddot{w}_0}{\partial y^3},
\end{aligned}
\tag{20b}
$$

$$
\begin{aligned}
& B_{11}\frac{\partial^3 u_0}{\partial x^3}+\left(B_{12}+2B_{66}\right)\frac{\partial^3 u_0}{\partial x\partial y^2}+\left(B_{12}+2B_{66}\right)\frac{\partial^3 v_0}{\partial x^2\partial y}+B_{22}\frac{\partial^3 v_0}{\partial y^3}-D_{11}\frac{\partial^4 w_0}{\partial x^4} \\
& -2\left(D_{12}+2D_{66}\right)\frac{\partial^4 w_0}{\partial x^2\partial y^2}-D_{22}\frac{\partial^4 w_0}{\partial y^4}+B_{11}^s\frac{\partial^5 u_0}{\partial x^5}+\left(B_{12}^s+B_{66}^s\right)\frac{\partial^5 u_0}{\partial x\partial y^4}+\left(B_{12}^s+B_{66}^s\right)\frac{\partial^5 v_0}{\partial x^4\partial y} \\
& +B_{22}^s\frac{\partial^5 v_0}{\partial y^5}+B_{66}^s\frac{\partial^5 v_0}{\partial x^3\partial y^2}+B_{66}^s\frac{\partial^5 v_0}{\partial x^2\partial y^3}-2D_{11}^s\frac{\partial^6 w_0}{\partial x^6}-2\left(D_{12}^s+2D_{66}^s\right)\frac{\partial^6 w_0}{\partial x^2\partial y^4} \\
& -2\left(D_{12}^s+2D_{66}^s\right)\frac{\partial^6 w_0}{\partial x^4\partial y^2}-2D_{22}^s\frac{\partial^6 w_0}{\partial y^6}-H_{11}^s\frac{\partial^8 w_0}{\partial x^8}-2\left(H_{12}^s+H_{66}^s\right)\frac{\partial^8 w_0}{\partial x^4\partial y^4} \\
& -H_{66}^s\frac{\partial^8 w_0}{\partial x^6\partial y^2}-H_{66}^s\frac{\partial^8 w_0}{\partial x^2\partial y^6}-H_{22}^s\frac{\partial^8 w_0}{\partial y^8}+A_{44}^s\frac{\partial^6 w_0}{\partial x^6}+A_{55}^s\frac{\partial^6 w_0}{\partial y^6}+q=I_0\ddot{w} \\
& +I_1\left(\frac{\partial\ddot{u}_0}{\partial x}+\frac{\partial\ddot{v}_0}{\partial y}\right)+J_1\left(\frac{\partial^3\ddot{u}_0}{\partial x^3}+\frac{\partial^3\ddot{v}_0}{\partial y^3}\right)-I_2\left(\frac{\partial^2\ddot{w}_0}{\partial x^2}+\frac{\partial^2\ddot{w}_0}{\partial y^2}\right) \\
& -2J_2\left(\frac{\partial^4\ddot{w}_0}{\partial x^4}+\frac{\partial^4\ddot{w}_0}{\partial y^4}\right)-K_2\left(\frac{\partial^6\ddot{w}_0}{\partial x^6}+\frac{\partial^6\ddot{w}_0}{\partial y^6}\right)
\end{aligned}
\tag{20c}
$$

## 3. Analytical solutions

The above equations of motion are analytically solved for bending and free vibration problems of a simply supported rectangular plate. Based on Navier solution procedure, the displacements are assumed as follows

$$
\begin{Bmatrix} u_0(x,y,t) \\ v_0(x,y,t) \\ w_0(x,y,t) \end{Bmatrix}=\sum_{m=1}^{\infty}\sum_{n=1}^{\infty}\begin{Bmatrix} U_{mn}\cos(\lambda\, x)\sin(\mu\, y)\, e^{i\,\omega\, t} \\ V_{mn}\sin(\lambda\, x)\cos(\mu\, y)\, e^{i\,\omega\, t} \\ W_{mn}\sin(\lambda\, x)\sin(\mu\, y)\, e^{i\,\omega\, t} \end{Bmatrix}
\tag{21}
$$

where $i=\sqrt{-1}$, $\lambda=m\pi/a$, $\mu=n\pi/b$, ($U_{mn}$, $V_{mn}$, $W_{mn}$) are the unknown maximum displacement coefficients, and $\omega$ is the angular frequency. The transverse load $q$ is also expanded in the double-Fourier sine series as

$$q(x,y)=\sum_{m=1}^{\infty}\sum_{n=1}^{\infty} q_{mn}\sin(\lambda\, x)\sin(\mu\, y) \tag{22}$$

For the case of a sinusoidally distributed load, we have

$$m=n=1 \qquad \text{and} \qquad q_{11}=q_0 \tag{23a}$$

For the case of a uniformly distributed load (UDL), it is

$$q_{mn}=\frac{16 q_0 ab}{\lambda\,\mu}, \qquad (m,n=1,3,5,......) \tag{23b}$$

where $q_0$ represents the intensity of the load at the plate centre.

Substituting Eqs. (21) and (22) into Eq. (20), the analytical solutions can be obtained from

$$\left(\begin{bmatrix} a_{11} & a_{12} & a_{13} \\ a_{12} & a_{22} & a_{23} \\ a_{13} & a_{23} & a_{33} \end{bmatrix} - \omega^2 \begin{bmatrix} m_{11} & 0 & m_{13} \\ 0 & m_{22} & m_{23} \\ m_{13} & m_{23} & m_{33} \end{bmatrix}\right)\begin{Bmatrix} U_{mn} \\ V_{mn} \\ W_{mn} \end{Bmatrix} = \begin{Bmatrix} 0 \\ 0 \\ q_{mn} \end{Bmatrix} \tag{24}$$

where

$$\begin{aligned}
a_{11} &= -\left(A_{11}\lambda^2 + A_{66}\mu^2\right)\\
a_{12} &= -\lambda\,\mu\left(A_{12}+A_{66}\right)\\
a_{13} &= \lambda\,[B_{11}\lambda^2 + (B_{12}+2B_{66})\,\mu^2 - B_{11}^s\lambda^4 - B_{12}^s\mu^4 - B_{66}^s\lambda^2\mu^2 - B_{66}^s\mu^4]\\
a_{22} &= -\left(A_{66}\lambda^2 + A_{22}\mu^2\right)\\
a_{23} &= \mu\,[B_{22}\mu^2 + (B_{12}+2B_{66})\,\lambda^2 - B_{22}^s\mu^4 - B_{12}^s\lambda^4 - B_{66}^s\lambda^2\mu^2 - B_{66}^s\lambda^4]\\
a_{33} &= -D_{11}\lambda^4 - 2(D_{12}+2D_{66})\lambda^2\mu^2 - D_{22}\mu^4 + 2(D_{11}^s\lambda^6 + D_{22}^s\mu^6)\\
&\quad + 2\left(\lambda^4\mu^2 + \lambda^2\mu^4\right)\left(D_{12}^s + 2D_{66}^s\right) - H_{11}^s\lambda^8 - H_{22}^s\mu^8 - 2\lambda^4\mu^4(H_{12}^s + H_{66}^s)\\
&\quad - \left(\lambda^6\mu^2 + \lambda^2\mu^6\right)H_{66}^s - A_{44}^s\lambda^6 - A_{55}^s\mu^6\\
m_{11} &= m_{22} = -I_0\\
m_{13} &= \lambda\left(I_1 + J_1\lambda^2\right)\\
m_{23} &= \mu\left(I_1 + J_1\mu^2\right),\\
m_{33} &= -\left(I_0 + I_2\left(\lambda^2+\mu^2\right) + 2J_2\left(\lambda^4+\mu^4\right) + K_2\left(\lambda^6+\mu^6\right)\right).
\end{aligned} \tag{25}$$

## 4. Evaluation of transverse stresses

In this approach the transverse stresses are obtained by integrating the equilibrium equation with respect to thickness direction. These relations can be expressed as

$$\tau_{zx} = \int_{-h/2}^{z} \left( \frac{\partial \sigma_x}{\partial x} + \frac{\partial \tau_{xy}}{\partial y} \right) dz \quad \text{and} \quad \tau_{yz} = \int_{-h/2}^{z} \left( \frac{\partial \tau_{xy}}{\partial x} + \frac{\partial \sigma_y}{\partial y} \right) dz \tag{26}$$

## 5. Numerical results

The general approach outlined in the previous sections for the bending and vibration analyses of the FG plates has been investigated through many numerical examples to verify the accuracy of the proposed three -unknown sinusoidal shear deformation theory. Two types of FG plates of $Al/Al_2O_3$ and $Al/ZrO_2$ are used in this study, and their corresponding material properties are listed in Table 1. The Young's modulus and density of FG plates (unless otherwise stated) are evaluated using the power law distribution (see Eq. (6)). The effective density $\rho(z)$ is estimated using the *power-law* distribution with Voigt's rule of mixtures as follows

$$\rho(z) = \rho_m + (\rho_c - \rho_m)\left( \frac{2z+h}{2h} \right)^k \tag{27}$$

For convenience, the following dimensionless forms are utilized

$$\begin{gathered}
\bar{z} = \frac{z}{h}, \quad S = a/h, \quad \bar{w} = \frac{10E_c}{q_0 a S^3} w\left(\frac{a}{2},\frac{b}{2},\bar{z}\right), \quad \hat{w} = \frac{100E}{q_0 h S^4} w\left(\frac{a}{2},\frac{b}{2},\bar{z}\right), \\
\bar{\sigma}_x = \frac{1}{q_0 S}\sigma_x\left(\frac{a}{2},\frac{b}{2},\bar{z}\right),\ \hat{\sigma}_x = \frac{1}{q_0 S^2}\sigma_x\left(\frac{a}{2},\frac{b}{2},\bar{z}\right),\ \bar{\sigma}_y = \frac{1}{q_0 S}\sigma_y\left(\frac{a}{2},\frac{b}{2},\bar{z}\right),\ \hat{\sigma}_y = \frac{1}{q_0 S^2}\sigma_y\left(\frac{a}{2},\frac{b}{2},\bar{z}\right), \\
\bar{\tau}_{xy} = \frac{1}{q_0 S}\tau_{xy}(0,0,\bar{z}),\ \hat{\tau}_{xy} = \frac{1}{q_0 S^2}\tau_{xy}(0,0,\bar{z}),\ \bar{\tau}_{yz} = \frac{1}{q_0 S}\tau_{yz}\left(\frac{a}{2},0,\bar{z}\right),\ \bar{\tau}_{xz} = \frac{1}{q_0 S}\tau_{xz}\left(0,\frac{b}{2},\bar{z}\right), \\
\hat{\omega} = \omega h\sqrt{\rho_c / E_c}, \quad \bar{\omega} = \omega \frac{a^2}{h}\sqrt{\rho_c / E_c}, \quad \bar{\beta} = \omega h\sqrt{\rho_m / E_m}
\end{gathered} \tag{28}$$

### *5.1 Bending analysis*

The first example is performed for square isotropic plate ($a/h$ = 10) subjected to UDL. The materials used for this example are as follows: the Young's modulus is $E$ = 210 GPa, and Poisson's ratio is $v$ = 0.3. The obtained results are compared with quasi-3D solutions given by Shimpi *et*

Table 1 Material properties used in the FG plate

| Properties | Metal aluminum (Al) | Ceramic | |
|---|---|---|---|
| | | Alumina ($Al_2O_3$) | Zirconia ($ZrO_2$) |
| $E$ (GPa) | 70 | 380 | 200 |
| $v$ | 0.3 | 0.3 | 0.3 |
| $\rho$ (kg/m$^3$) | 2702 | 3800 | 5700 |

Table 2 The dimensionless stresses and transversal displacement for isotropic square plate ($a$ / $h$ = 10) subjected to a UDL

| Theory | $\hat{w}(a/2,b/2,0)$ | $\hat{\sigma}_x(h/2)$ | $\hat{\sigma}_y(h/2)$ | $\hat{\tau}_{xy}(h/2)$ | $\bar{\tau}_{xz}(0,b/2,0)$ | $\bar{\tau}_{yz}(a/2,0,0)$ |
|---|---|---|---|---|---|---|
| Present | 4.6183 | 0.2922 | 0.2922 | 0.1962 | 0.4234 | 0.4234 |
| Shimpi *et al*. (2003) | 4.625 | 0.307 | 0.307 | 0.195 | 0.505 | 0.505 |
| Srinivas *et al*. (1970) | 4.639 | 0.290 | 0.290 | / | 0.488 | / |
| Hebali *et al*. (2014) | 4.631 | 0.276 | 0.276 | 0.197 | 0.481 | 0.481 |

*al*. (2003), Hebali *et al*. (2014) and the exact solution carried out by Srinivas *et al*. (1970). It can be seen from Table 2 that the dimensionless displacement and stresses predicted by the new proposed theory with three unknowns are in good agreement with those generated by the quasi-3D solutions (Shimpi *et al*. 2003, Hebali *et al*. 2014) and the exact 3D solution (Srinivas *et al*. 1970).

Table 3 The dimensionless in-plane longitudinal stress $\bar{\sigma}_x$ and displacement $\bar{w}$ for FG square plate subjected to a sinusoidal load

| $k$ | Theory | $\bar{\sigma}_x(h/3)$ | | | $\bar{w}(a/2,b/2,0)$ | | |
|---|---|---|---|---|---|---|---|
| | | $a/h=4$ | $a/h=10$ | $a/h=100$ | $a/h=4$ | $a/h=10$ | $a/h=100$ |
| 1 | Carrera *et al*. (2011) $\varepsilon_z=0$ | 0.7856 | 2.0068 | 20.149 | 0.7289 | 0.5890 | 0.5625 |
| | Carrera *et al*. (2011) $\varepsilon_z\neq0$ | 0.6221 | 1.5064 | 14.969 | 0.7171 | 0.5875 | 0.5625 |
| | Neves *et al*. (2012) $\varepsilon_z\neq0$ | 0.5925 | 1.4945 | 14.969 | 0.6997 | 0.5845 | 0.5624 |
| | Present $\varepsilon_z=0$ | 0.6073 | 1.5073 | 14.969 | 0.7224 | 0.5860 | 0.5625 |
| 4 | Carrera *et al*. (2011) $\varepsilon_z=0$ | 0.5986 | 1.5874 | 16.047 | 1.1673 | 0.8828 | 0.8286 |
| | Carrera *et al*. (2011) $\varepsilon_z\neq0$ | 0.4877 | 1.1971 | 11.923 | 1.1585 | 0.8821 | 0.8286 |
| | Neves *et al*. (2012) $\varepsilon_z\neq0$ | 0.4404 | 1.1783 | 11.932 | 1.1178 | 0.8750 | 0.8286 |
| | Present $\varepsilon_z=0$ | 0.4976 | 1.2046 | 11.924 | 1.1058 | 0.8671 | 0.8285 |
| 10 | Carrera *et al*. (2011) $\varepsilon_z=0$ | 0.4345 | 1.1807 | 11.989 | 1.3925 | 1.0090 | 0.9361 |
| | Carrera *et al*. (2011) $\varepsilon_z\neq0$ | 0.1478 | 0.8965 | 8.9077 | 1.3745 | 1.0072 | 0.9361 |
| | Neves *et al*. (2012) $\varepsilon_z\neq0$ | 0.3227 | 1.1783 | 11.932 | 1.3490 | 0.8750 | 0.8286 |
| | Present $\varepsilon_z=0$ | 0.3786 | 0.9019 | 8.9084 | 1.2723 | 0.9816 | 0.9359 |

The second example deals with thin and thick $Al_2O_3$ square plates subjected to a sinusoidal load. Three different values of the power law index are considered: $k$ = 1, 4, and 10. Table 3 contains nondimensional transverse displacement $\overline{w}$ and axial stress $\overline{\sigma}_x$. The obtained results are compared with quasi-3D solutions given by Neves *et al*. (2012) and Hebali *et al*. (2014), and with those obtained using finite-element approximations by Carrera *et al*. (2011). In general, a good agreement between the results is found. The small difference between the results is due to the effect of thickness stretching which is considered in quasi-3D solutions (Neves *et al*. 2012, Hebali *et al*. 2014).

In the third example, a moderately thick $Al/Al_2O_3$ square plate ($a / h$ = 10) subjected to a sinusoidal load is examined. Table 4 shows the effects of power law index $k$ on the dimensionless displacements and stresses. The present results are compared with the results of the sinusoidal shear deformation theory (SSDT) for FG plates presented by Zenkour (2006). In general, the obtained results are almost identical with those reported by Zenkour (2006) based on SSDT for all cases.

It should be noted that the present theory involves three unknowns as against five or more unknowns in other higher order shear deformation theory. This indicates that the proposed three-unknown sinusoidal shear deformation theory can improve the computational cost due to reducing the number of unknowns as well as governing equations of motion.

To further prove the accuracy of present three -unknown sinusoidal shear deformation theory for wide range of thickness ratio $a / h$, the variation of dimensionless deflection $\overline{w}$ versus the thickness ratio $a / h$ is illustrated in Fig. 2. The obtained results are compared with those computed using the third-order shear deformation theory (TSDT) of Reddy (2000) and the CPT. In general, the results of present theory and TSDT are almost identical. Since the CPT neglects the shear deformation effects, it underestimates deflection of thick plate.

The through thickness variation for stresses ($\overline{\sigma}_x$ and $\overline{\tau}_{xy}$) is also presented in Fig. 3 for the case of $k$ = 2. The obtained results are compared with those computed using TSDT where a good agreement is showed.

Table 4 Effects of volume fraction exponent on the dimensionless stresses and deflections of a FG square plate subjected to a sinusoidal load

| $k$ | $\overline{w}$ | | $\overline{\sigma}_x$ | | $\overline{\tau}_{xz}$ | | $\overline{\tau}_{xy}$ | |
|---|---|---|---|---|---|---|---|---|
| | Present | SSDT[(a)] | Present | SSDT[(a)] | Present | SSDT[(a)] | Present | SSDT[(a)] |
| Ceramic | 0.2930 | 0.2960 | 2.0139 | 1.9955 | 0.2416 | 0.2462 | 0.7174 | 0.7065 |
| 1 | 0.5860 | 0.5889 | 3.1076 | 3.0870 | 0.2408 | 0.2462 | 0.6179 | 0.6110 |
| 2 | 0.7517 | 0.7573 | 3.6351 | 3.6094 | 0.2285 | 0.2265 | 0.5513 | 0.5441 |
| 3 | 0.8276 | 0.8377 | 3.9043 | 3.8742 | 0.2230 | 0.2107 | 0.5614 | 0.5525 |
| 4 | 0.8671 | 0.8819 | 4.1023 | 4.0693 | 0.2214 | 0.2029 | 0.5772 | 0.5667 |
| 5 | 0.8930 | 0.9118 | 4.2843 | 4.2488 | 0.2209 | 0.2017 | 0.5869 | 0.5755 |
| 6 | 0.9137 | 0.9356 | 4.4624 | 4.4244 | 0.2208 | 0.2041 | 0.5924 | 0.5803 |
| 7 | 0.9321 | 0.9562 | 4.6378 | 4.5971 | 0.2208 | 0.2081 | 0.5958 | 0.5834 |
| 8 | 0.9493 | 0.9750 | 4.8096 | 4.7661 | 0.2207 | 0.2124 | 0.5982 | 0.5856 |
| 9 | 0.9658 | 0.9925 | 4.9765 | 4.9303 | 0.2207 | 0.2164 | 0.6003 | 0.5875 |
| 10 | 0.9816 | 1.0089 | 5.1378 | 5.0890 | 0.2207 | 0.2198 | 0.6022 | 0.5894 |
| Metal | 1.5909 | 1.6070 | 2.0139 | 1.9955 | 0.2416 | 0.2462 | 0.7174 | 0.7065 |

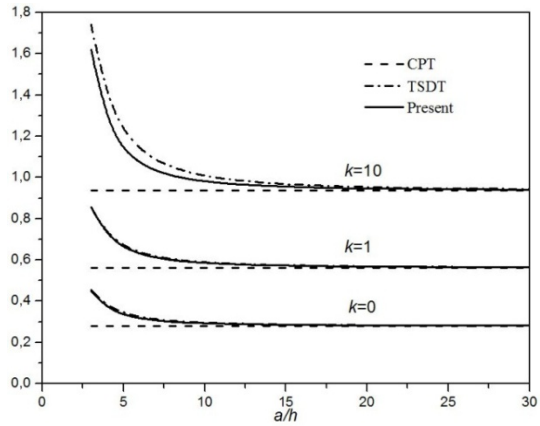


Fig. 2 Variation of dimensionless deflection $\overline{w}$ of isotropic Al/$Al_2O_3$ square plates under sinusoidal loads versus thickness ratio $a / h$

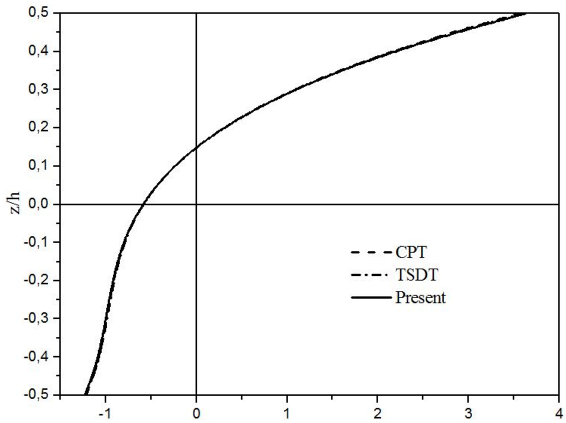


(a)

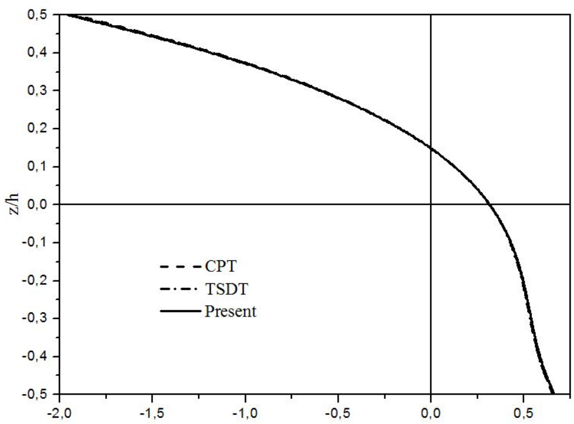


(b)

Fig. 3 Variation of dimensionless stresses ($\overline{\sigma}_x$ and $\overline{\tau}_{xy}$) of isotropic Al/$Al_2O_3$ square plates under sinusoidal loads ($a / h$ = 10 and $k$ = 2)

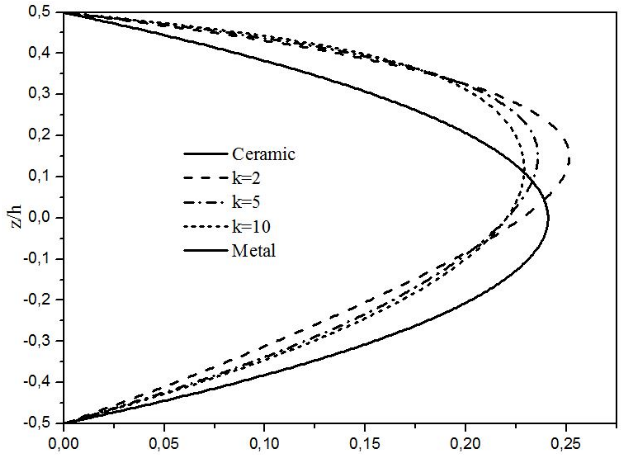


Fig. 4 Variation of dimensionless transverse stress $(\bar{\tau}_{xz})$ of isotropic $Al/Al_2O_3$ square plates under sinusoidal loads ($a$ / $h$ = 10 and $k$ = 2)

In Fig. 4 we have plotted the through-the-thickness distributions of the transverse shear stress $\bar{\tau}_{xz}$. The through-the-thickness distributions of the transverse shear stresses for FG plates are not parabolic as in the case of homogeneous metal or ceramic beams.

### *5.2 Free vibration analysis*

The accuracy of the new proposed three -unknown sinusoidal shear deformation theory is also verified with free vibration analysis.

The first verification is performed for thin and thick $Al/ZrO_2$ square plates. This example aims to verify the obtained results with the 3D solutions of Vel and Batra (2004) and quasi-3D solution of Belabed *et al*. (2014). Young's modulus is evaluated using Mori–Tanaka scheme (see Eq. (7)). This approach has also been used by many other investigators and is applicable in zones of graded microstructure which possess a well-defined continuous matrix and a discontinuous particulate phase. It models with sufficient robustness the interaction of the elastic fields among neighboring inclusions. The non-dimensional fundamental frequency $\bar{\beta}$ is given in Table 5 for different values of thickness ratio and power law index. It can be seen that the obtained results agree well with the 3D solutions (Vel and Batra 2004) and quasi-3D solutions (Belabed *et al*. 2014).

The next verification is performed for thin and thick $Al/Al_2O_3$ square plates with thickness ratio varied from 5 to 20 and power law index varied from 0 to 10. The non-dimensional frequencies

Table 5 Non-dimensional fundamental frequency $\bar{\beta}$ of $Al/ZrO_2$ square plates

| Method | $k = 0$ | | $k = 1$ | | | $a/h = 5$ | | |
|---|---|---|---|---|---|---|---|---|
| | $a/h = \sqrt{10}$ | $a/h = 10$ | $a/h = 5$ | $a/h = 10$ | $a/h = 20$ | $k = 2$ | $k = 3$ | $k = 5$ |
| 3D[(a)] | 0.4658 | 0.0578 | 0.2192 | 0.0596 | 0.0153 | 0.2197 | 0.2211 | 0.2225 |
| Quasi-3D[(b)] | 0.4659 | 0.0578 | 0.2192 | 0.0597 | 0.0153 | 0.2201 | 0.2214 | 0.2225 |
| Present | 0.4633 | 0.0580 | 0.2190 | 0.0595 | 0.0152 | 0.2209 | 0.2231 | 0.2250 |

Table 6 Non-dimensional fundamental frequency $\hat{\omega}$ of Al/Al$_2$O$_3$ square plates

| $a$ / $h$ | Method | $k$ | | | | |
|---|---|---|---|---|---|---|
| | | 0 | 0.5 | 1 | 4 | 10 |
| 5 | Quasi-3D[a] | 0.2121 | 0.1819 | 0.1640 | 0.1383 | 0.1306 |
| | TSDT[b] | 0.2113 | 0.1807 | 0.1631 | 0.1378 | 0.1301 |
| | FSDT[c] | 0.2112 | 0.1805 | 0.1631 | 0.1397 | 0.1324 |
| | Present | 0.2133 | 0.1815 | 0.1637 | 0.1401 | 0.1342 |
| 10 | Quasi-3D[a] | 0.0578 | 0.0494 | 0.0449 | 0.0389 | 0.0368 |
| | TSDT[b] | 0.0577 | 0.0490 | 0.0442 | 0.0381 | 0.0364 |
| | FSDT[c] | 0.0577 | 0.0490 | 0.0442 | 0.0382 | 0.0366 |
| | Present | 0.0580 | 0.0491 | 0.0443 | 0.0384 | 0.0368 |
| 20 | Quasi-3D[a] | 0.0148 | 0.0126 | 0.0115 | 0.0100 | 0.0095 |
| | TSDT[b] | 0.0148 | 0.0125 | 0.0113 | 0.0098 | 0.0094 |
| | FSDT[c] | 0.0148 | 0.0125 | 0.0113 | 0.0098 | 0.0094 |
| | Present | 0.0148 | 0.0126 | 0.0113 | 0.0098 | 0.0094 |

[a] Taken from Belabed *et al*. (2014); [b] Taken from Hosseini-Hashemi *et al*. (2011a);
[c] Taken from Hosseini-Hashemi *et al*. (2011b)

Table 7 Comparison of frequency parameter $\overline{\varpi}$ of AL/Al$_2$O$_3$ rectangular plate ($b$ = 2$a$)

| $a$ / $h$ | Mode no ($m$, $n$) | Method | $k$ | | | | | | |
|---|---|---|---|---|---|---|---|---|---|
| | | | 0 | 0.5 | 1 | 2 | 5 | 8 | 10 |
| 5 | 1 (1,1) | FSDT[a] | 3.4409 | 2.9322 | 2.6473 | 2.4017 | 2.2528 | 2.1985 | 2.1677 |
| | | $n$-order theory[b] | 3.4412 | 2.9346 | 2.6475 | 2.3948 | 2.2271 | 2.1696 | 2.1406 |
| | | Present | 3.4649 | 2.9538 | 2.6651 | 2.4095 | 2.2517 | 2.2024 | 2.1748 |
| | 2 (1,2) | FSDT[a] | 5.2802 | 4.5122 | 4.0773 | 3.6953 | 3.4492 | 3.3587 | 3.3094 |
| | | $n$-order theory[b] | 5.2813 | 4.5179 | 4.0780 | 3.6805 | 3.3938 | 3.2964 | 3.2513 |
| | | Present | 5.3318 | 4.5376 | 4.0915 | 3.7012 | 3.4677 | 3.3957 | 3.3543 |
| | 3 (1,3) | FSDT[a] | 8.0710 | 6.9231 | 6.2636 | 5.6695 | 5.2579 | 5.1045 | 5.0253 |
| | | $n$-order theory[b] | 8.0748 | 6.9366 | 6.2662 | 5.6389 | 5.1424 | 4.9757 | 4.9055 |
| | | Present | 8.1706 | 7.0160 | 6.3398 | 5.6981 | 5.2376 | 5.1050 | 5.0411 |
| 10 | 1 (1,1) | FSDT[a] | 3.6518 | 3.0983 | 2.7937 | 2.5386 | 2.3998 | 2.3504 | 2.3197 |
| | | $n$-order theory[b] | 3.6517 | 3.0990 | 2.7936 | 2.5364 | 2.3916 | 2.3410 | 2.3110 |
| | | Present | 3.6597 | 3.1042 | 2.7982 | 2.5408 | 2.4014 | 2.3541 | 2.3244 |
| | 2 (1,2) | FSDT[a] | 5.7693 | 4.8997 | 4.4192 | 4.0142 | 3.7881 | 3.7072 | 3.6580 |
| | | $n$-order theory[b] | 5.7694 | 4.9014 | 4.4192 | 4.0089 | 3.7682 | 3.6845 | 3.6368 |
| | | Present | 5.7972 | 4.9149 | 4.4294 | 4.0224 | 3.8042 | 3.7304 | 3.6839 |
| | 3 (1,3) | FSDT[a] | 9.1876 | 7.8145 | 7.0512 | 6.4015 | 6.0247 | 5.8887 | 5.8086 |
| | | $n$-order theory[b] | 9.1880 | 7.8189 | 7.0514 | 6.3886 | 5.9764 | 5.8340 | 5.7574 |
| | | Present | 9.2432 | 7.8494 | 7.0762 | 6.4166 | 6.0461 | 5.9246 | 5.8509 |

[a] Taken from Hosseini-Hashemi *et al*. (2011b); [b] Taken from Klouche Djedid *et al*. (2014)

$\hat{\varpi}$ predicted by the quasi-3D solution of Belabed *et al*. (2014), the third shear deformation theory (TSDT) (Hosseini-Hashemi *et al*. 2011a), FSDT (Hosseini-Hashemi *et al*. 2011b), and the present theory are compared in Table 6. It can be seen from Table 6 that the computations based on the present theory are once again in excellent agreement with those predicted by the other shear deformations theories. It is emphasized that the TSDT, FSDT and the quasi-3D solutions contain a greater number of unknowns than those associated with the present theory.

The last example is carried out for rectangular $Al/Al_2O_3$ plate ($b$ = 2$a$). The lowest three frequency parameters $\overline{\varpi}$ obtained from present theory are compared with those reported by Hosseini-Hashemi *et al*. (2011b) based on FSDT and by Klouche Djedid *et al*. (2014) based on simple $n$-order four variable refined theory in Table 7. Again, it can be seen that the results obtained by present theory are in good agreement with those reported by Hosseini-Hashemi *et al*. (2011b) based on FSDT, and Klouche Djedid *et al*. (2014) based on simple $n$-order four variable refined theory.

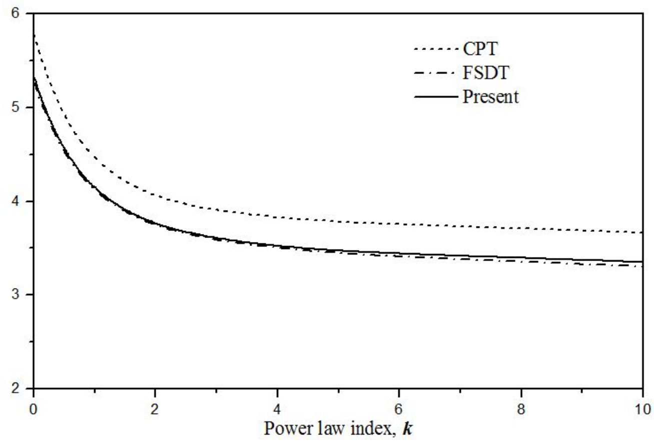


Fig. 5 Variation of dimensionless fundamental frequency $\overline{\varpi}$ of isotropic $Al/Al_2O_3$ square plates under sinusoidal loads versus power law index $k$ ($a/h$ = 5)

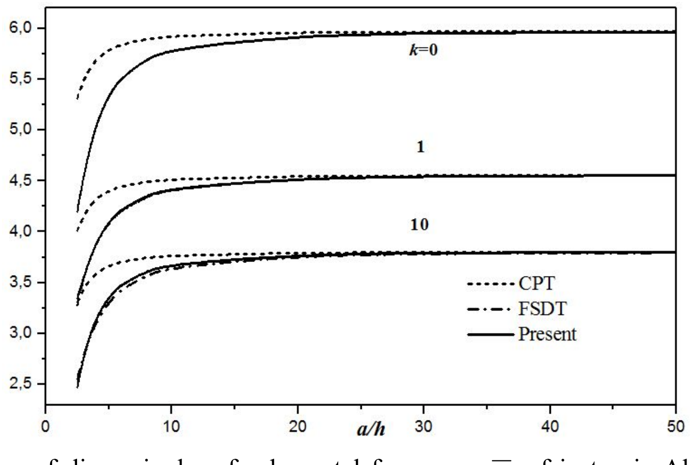


Fig. 6 Variation of dimensionless fundamental frequency $\overline{\varpi}$ of isotropic $Al/Al_2O_3$ square plates under sinusoidal loads versus thickness ratio $a/h$

The variations of the nondimensional fundamental natural frequency $\bar{\omega}$ versus the power law index $k$ and the thickness ratio $a / h$ are presented in Figs. 5 and 6, respectively, where the present results are compared with those predicted by both FSDT and CPT. It should be noted that the developed three -unknown sinusoidal shear deformation theory contains less number of unknowns than the FSDT.

It can be concluded that the present theory not only gives comparable results with the existing higher-order and first shear deformations theories, but also is simpler than the existing HSDT and FSDT due to having less number of unknowns, i.e., three as against five. From the results can be concluded also that due to the accuracy of the present theory and its reduced number of unknowns, this work opens a new generation of higher order shear deformation theory not available in the literature with potential for further investigation due to it similarities with the CPT and FSDT.

## 6. Conclusions

A new simple and accurate 3-unknowns sinusoidal shear deformation theory is developed for the bending and vibration analysis of FG plates. The interesting advantage of this theory is that, in addition to including the shear deformation effect, the displacement field is modelled with only 3 unknowns as the case of the classical plate theory (CPT) and which is even less than the first order shear deformation theory (FSDT). Results prove that the present theory is capable to predict accurate results compared with the CPT, FSDT and other HSDTs with higher number of unknowns and so deserve special attention and offer potential for future research.

## References

Ait Amar Meziane, M., Abdelaziz, H.H. and Tounsi, A. (2014), "An efficient and simple refined theory for buckling and free vibration of exponentially graded sandwich plates under various boundary conditions", *J. Sandw. Struct. Mater.*, **16**(3), 293-318.

Ait Atmane, H., Tounsi, A., Bernard, F. and Mahmoud, S.R. (2015), "A computational shear displacement model for vibrational analysis of functionally graded beams with porosities", *Steel Compos. Struct., Int. J.*, **19**(2), 369-384.

Ait Yahia, S., Ait Atmane, H., Houari, M.S.A. and Tounsi, A. (2015), "Wave propagation in functionally graded plates with porosities using various higher-order shear deformation plate theories", *Struct. Eng. Mech., Int. J.*, **53**(6), 1143-1165.

Akavci, S.S. (2015), "An efficient shear deformation theory for free vibration of functionally graded thick rectangular plates on elastic foundation", *Compos. Struct.*, **108**, 667-676.

Akbaş, Ş.D. (2015), "Wave propagation of a functionally graded beam in thermal environments", *Steel Compos. Struct., Int. J.*, **19**(6), 1421-1447.

Al-Basyouni, K.S., Tounsi, A. and Mahmoud, S.R. (2015), "Size dependent bending and vibration analysis of functionally graded micro beams based on modified couple stress theory and neutral surface position", *Compos. Struct.*, **125**, 621-630.

Amirpour, M., Das, R. and Saavedra Flores, E.I. (2016), "Analytical solutions for elastic deformation of functionally graded thick plates with in-plane stiffness variation using higher order shear deformation theory", *Compos. Part B: Eng.*, **94**, 109-121.

Arefi, M. (2015), "Elastic solution of a curved beam made of functionally graded materials with different cross sections", *Steel Compos. Struct., Int. J.*, **18**(3), 659-672.

Attia, A., Tounsi, A., Adda Bedia, E.A. and Mahmoud, S.R. (2015), "Free vibration analysis of functionally graded plates with temperature-dependent properties using various four variable refined plate theories", *Steel Compos. Struct., Int. J.*, **18**(1), 187-212.

Aydogdu, M. (2006), “Comparison of various shear deformation theories for bending, buckling, and vibration of rectangular symmetric cross-ply plate with simply supported edges”, *J. Compos. Mater.*, **40**(23), 2143-2155.

Bachir Bouiadjra, R., Adda Bedia, E.A. and Tounsi, A. (2013), “Nonlinear thermal buckling behavior of functionally graded plates using an efficient sinusoidal shear deformation theory”, *Struct. Eng. Mech., Int. J.*, **48**(4), 547-567.

Belabed, Z., Houari, M.S.A., Tounsi, A., Mahmoud, S.R. and Anwar Bég, O. (2014), “An efficient and simple higher order shear and normal deformation theory for functionally graded material (FGM) plates”, *Compos.: Part B*, **60**, 274-283.

Beldjelili, Y., Tounsi, A. and Mahmoud, S.R. (2016), “Hygro-thermo-mechanical bending of S-FGM plates resting on variable elastic foundations using a four-variable trigonometric plate theory”, *Smart Struct. Syst., Int. J.*, **18**(4), 755-786.

Bellifa, H., Benrahou, K.H., Hadji, L., Houari, M.S.A. and Tounsi, A. (2016), “Bending and free vibration analysis of functionally graded plates using a simple shear deformation theory and the concept the neutral surface position”, *J. Braz. Soc. Mech. Sci. Eng.*, **38**(1), 265-275.

Belkorissat, I., Houari, M.S.A., Tounsi, A., Adda Bedia, E.A. and Mahmoud, S.R. (2015), “On vibration properties of functionally graded nano-plate using a new nonlocal refined four variable model”, *Steel Compos. Struct., Int. J.*, **18**(4), 1063-1081.

Bennai, R., Ait Atmane, H. and Tounsi, A. (2015), “A new higher-order shear and normal deformation theory for functionally graded sandwich beams”, *Steel Compos. Struct., Int. J.*, **19**(3), 521-546.

Bennoun, M., Houari, M.S.A. and Tounsi, A. (2016), “A novel five variable refined plate theory for vibration analysis of functionally graded sandwich plates”, *Mech. Adv. Mater. Struct.*, **23**(4), 423-431.

Benveniste. Y. (1987), “A new approach to the application of Mori-Tanaka’s theory in composite materials”, *Mech. Mat.*, **6**(2), 147-157.

Bouchafa, A., Bachir Bouiadjra, M., Houari, M.S.A. and Tounsi, A. (2015), “Thermal stresses and deflections of functionally graded sandwich plates using a new refined hyperbolic shear deformation theory”, *Steel Compos. Struct., Int. J.*, **18**(6), 1493-1515.

Bouderba, B., Houari, M.S.A. and Tounsi, A. (2013), “Thermomechanical bending response of FGM thick plates resting on Winkler–Pasternak elastic foundations”, *Steel Compos. Struct., Int. J.*, **14**(1), 85-104.

Bouderba, B., Houari, M.S.A. and Tounsi, A. and Mahmoud, S.R. (2016), “Thermal stability of functionally graded sandwich plates using a simple shear deformation theory”, *Struct. Eng. Mech., Int. J.*, **58**(3), 397-422.

Boukhari, A., Atmane, H., Tounsi, A., Adda Bedia, E. and Mahmoud, S. (2016), “An efficient shear deformation theory for wave propagation of functionally graded material plates”, *Struct. Eng. Mech., Int. J.*, **57**(5), 837-859.

Bounouara, F., Benrahou, K.H., Belkorissat, I. and Tounsi, A. (2016), “A nonlocal zeroth-order shear deformation theory for free vibration of functionally graded nanoscale plates resting on elastic foundation”, *Steel Compos. Struct., Int. J.*, **20**(2), 227-249.

Bourada, M., Kaci, A., Houari, M.S.A. and Tounsi, A. (2015), “A new simple shear and normal deformations theory for functionally graded beams”, *Steel Compos. Struct., Int. J.*, **18**(2), 409-423.

Bourada, F., Amara, K. and Tounsi, A. (2016), “Buckling analysis of isotropic and orthotropic plates using a novel four variable refined plate theory”, *Steel Compos. Struct., Int. J.*, **21**(6), 1287-1306.

Bousahla, A.A., Houari, M.S.A., Tounsi, A. and Adda Bedia, E.A. (2014), “A novel higher order shear and normal deformation theory based on neutral surface position for bending analysis of advanced composite plates”, *Int. J. Computat. Method.*, **11**(6), 1350082.

Bousahla, A.A., Benyoucef, S. Tounsi, A. and Mahmoud, S.R. (2016), “On thermal stability of plates with functionally graded coefficient of thermal expansion”, *Struct. Eng. Mech., Int. J.*, **60**(2), 313-335.

Carrera, E., Brischetto, S., Cinefra, M. and Soave, M. (2011), “Effects of thickness stretching in functionally graded plates and shells”, *Compos., Part B*, **42**(2), 123-133.

Darılmaz, K. (2015), “Vibration analysis of functionally graded material (FGM) grid systems”, *Steel*

*Compos*. *Struct*., *Int*. *J*., **18**(2), 395-408.
Draiche, K., Tounsi, A. and Khalfi, Y. (2014), "A trigonometric four variable plate theory for free vibration of rectangular composite plates with patch mass", *Steel Compos*. *Struct*., *Int*. *J*., **17**(1), 69-81.
Hamidi, A., Houari, M.S.A., Mahmoud, S.R. and Tounsi, A. (2015), "A sinusoidal plate theory with 5-unknowns and stretching effect for thermomechanical bending of functionally graded sandwich plates", *Steel Compos*. *Struct*., *Int*. *J*., **18**(1), 235-253.
Hebali, H., Tounsi, A., Houari, M.S.A., Bessaim, A. and Adda Bedia, E.A. (2014), "A new quasi-3D hyperbolic shear deformation theory for the static and free vibration analysis of functionally graded plates", *ASCE J*. *Eng*. *Mech*., **140**(2), 374-383.
Hosseini-Hashemi, S., Fadaee, M. and Atashipour, S.R. (2011a), "Study on the free vibration of thick functionally graded rectangular plates according to a new exact closed-form procedure", *Compos*. *Struct*., **93**(2), 722-735.
Hosseini-Hashemi, S., Fadaee, M. and Atashipour, S.R. (2011b), "A new exact analytical approach for free vibration of Reissner-Mindlin functionally graded rectangular plates", *Int*. *J*. *Mech*. *Sci*., **53**(1), 11-22.
Jha, D.K., Kant, T. and Singh, R.K. (2013), "Free vibration response of functionally graded thick plates with shear and normal deformations effects", *Compos*. *Struct*., **96**, 799-823.
Kant, T. and Pandya, B.N. (1988), "A simple finite element formulation of a higher-order theory for unsymmetrically laminated composite plates", *Compos*. *Struct*., **9**(3), 215-246.
Kar, V.R. and Panda, S.K. (2015a), "Nonlinear flexural vibration of shear deformable functionally graded spherical shell panel", *Steel Compos*. *Struct*., *Int*. *J*., **18**(3), 693-709.
Kar, V.R. and Panda, S.K. (2015b), "Free vibration responses of temperature dependent functionally graded curved panels under thermal environment", *Latin Am*. *J*. *Solid*. *Struct*., **12**(11), 2006-2024.
Kar, V.R. and Panda, S.K. (2016), "Thermal buckling and vibration analysis of laminated composite curved shell panel", *Aircraft Eng*. *Aerosp*. *Technol*.: *Int*. *J*., **88**(1), 97-107.
Karama, M., Afaq, K.S. and Mistou, S. (2003), "Mechanical behaviour of laminated composite beam by the newmulti-layered laminated composite structures model with transverse shear stress continuity", *Int*. *J*. *Solids Struct*., **40**(6), 1525-1546.
Khalfi, Y., Houari, M.S.A. and Tounsi, A. (2014), "A Refined and Simple Shear Deformation Theory for Thermal Buckling of Solar Functionally Graded Plates on Elastic Foundation", *Int*. *J*. *Computat*. *Method*., **11**(5), 1350077.
Kitipornchai, S., Yang, J. and Liew, K.M. (2006), "Random vibration of the functionally graded laminates in thermal environments", *Compos*. *Meth*. *Appl*. *Mech*. *Eng*., **195**(9-12), 1075-1095.
Klouche Djedid, I., Benachour, A., Houari, M.S.A. and Tounsi, A. (2014), "A *n*-order four variable refined theory for bending and free vibration of functionally graded plates", *Steel Compos*. *Struct*., *Int*. *J*., **17**(1), 21-46.
Koizumi, M. (1993), "The concept of FGM", *Ceram*. *Trans*. *Funct*. *Grad*. *Mater*., **34**, 3-10.
Larbi Chaht, F., Kaci, A., Houari, M.S.A., Tounsi, A., Anwar Bég, O. and Mahmoud, S.R. (2015), "Bending and buckling analyses of functionally graded material (FGM) size-dependent nanoscale beams including the thickness stretching effect", *Steel Compos*. *Struct*., *Int*. *J*., **18**(2), 425-442.
Mahapatra, T.R., Kar, V.R. and Panda, S.K. (2016a), "Large amplitude free vibration analysis of laminated composite spherical panel under hygrothermal environment", *Int*. *J*. *Struct*. *Stabil*. *Dyn*., **16**(3), 1450105.
Mahapatra, T.R., Panda, S.K. and Kar, V.R. (2016b), "Nonlinear flexural analysis of laminated composite panel under hygro-thermo-mechanical loading: A micromechanical approach", *Int*. *J*. *Struct*. *Stabil*. *Dyn*., **13**(3), 1650015.
Mahapatra, T.R., Kar, V.R. and Panda, S.K. (2016c), "Large amplitude bending behaviour of laminated composite curved panels", *Eng*. *Computat*., **33**(1), 116-138.
Mahi, A., Adda Bedia, E.A. and Tounsi, A. (2015), "A new hyperbolic shear deformation theory for bending and free vibration analysis of isotropic, functionally graded, sandwich and laminated composite plates", *Appl*. *Math*. *Modelling*, **39**(9), 2489-2508.
Mantari, J.L., Ramos, I.A., Carrera, E. and Petrolo, M. (2016), "Static analysis of functionally graded plates using new non-polynomial displacement fields via Carrera Unified Formulation", *Compos*. *Part B*., **89**,

127-142.

Meradjah, M., Kaci, A., Houari, M.S.A., Tounsi, A. and Mahmoud, S.R. (2015), "A new higher order shear and normal deformation theory for functionally graded beams", *Steel Compos. Struct., Int. J.*, **18**(3), 793-809.

Mori, T. and Tanaka. K. (1973), "Average stress in matrix and average elastic energy of materials with misfitting inclusions", *Acta Metall*, **21**(5), 571-574.

Neves, A.M.A., Ferreira, A.J.M., Carrera, E., Rogue, C.M.E., Cinefra, M., Jorge, R.M.N. and Soares, C.M.M. (2012), "A quasi-3D sinusoidal shear deformation theory for the static and free vibration analysis of functionally graded plates", *Compos. Part B*, **43**(2), 711-725.

Pandya, B.N. and Kant, T. (1988), "Finite element analysis of laminated composite plates using a higher-order displacementmodel", *Compos. Sci. Technol.*, **32**(2), 137-155.

Pradyumna, S. and Bandyopadhyay, J.N. (2008), "Free vibration analysis of functionally graded curved panels using a higher-order finite element formulation", *J. Sound Vib.*, **318**(1-2), 176-192.

Reddy, J.N. (1984), "A simple higher-order theory for laminated composite plates", *J. Appl. Mech.*, **51**(4), 745-752.

Reddy, J.N. (2000), "Analysis of functionally graded plates", *Int. J. Numer. Methods Eng.*, **47**(1-3), 663-684.

Ren, J.G. (1986), "A new theory of laminated plate", *Compos. Sci. Technol.*, **26**(3), 225-239.

Sahoo, S.S., Panda, S.K. and Mahapatra, T.R. (2016a), "Static, free vibration and transient response of laminated composite curved shallow panel – An experimental approach", *Eur. J. Mech. - A/Solids*, **59**, 95-113.

Sahoo, S.S., Panda, S.K. and Sen, D. (2016b), "Effect of delamination on static and dynamic behavior of laminated composite plate", *AIAA J.*, **54**(8), 2530-2544.

Shimpi, R.P., Arya, H. and Naik, N.K. (2003), "A higher order displacement model for the plate analysis", *J. Reinf. Plast. Comp.*, **18**(22), 1667-1688.

Soldatos, K.P. (1992), "A transverse shear deformation theory for homogeneous monoclinic plates", *Acta Mech.*, **94**(3), 195-220.

Srinivas, S., Joga, C.V. and Rao, A.K. (1970), "Bending, vibration and buckling of simply supported thick orthotropic rectangular plate and laminates", *Int. J. Solids Struct.*, **6**(11), 1463-1481.

Touratier, M. (1991), "An efficient standard plate theory", *Int. J. Eng. Sci.*, **29**(8), 901-916.

Tounsi, A., Houari, M.S.A., Benyoucef, S. and Adda Bedia, E.A. (2013), "A refined trigonometric shear deformation theory for thermoelastic bending of functionally graded sandwich plates", *Aerosp. Sci. Technol.*, **24**(1), 209-220.

Tounsi, A., Houari, M.S.A. and Bessaim, A. (2016), "A new 3-unknowns non-polynomial plate theory for buckling and vibration of functionally graded sandwich plate", *Struct. Eng. Mech., Int. J.*, (Accepted)

Vel, S.S. and Batra, R.C. (2004), "Three-dimensional exact solution for the vibration of functionally graded rectangular plates", *J. Sound Vib.*, **272**(3-5), 703-730.

Yaghoobi, H. and Yaghoobi, P. (2013), "Buckling analysis of sandwich plates with FGM face sheets resting on elastic foundation with various boundary conditions: An analytical approach", *Meccanica*, **48**(8), 2019-2035.

Yang, J., Liew, K.M. and Kitipornchai, S. (2005), "Stochastic analysis of compositionally graded plates with system randomness under static loading", *Int. J. Mech. Sci.*, **47**(10), 1519-1541.

Zhao, X., Lee, Y.Y. and Liew, K.M. (2009), "Free vibration analysis of functionally graded plates using the element-free kp-Ritz method", *J. Sound Vib.*, **319**(3-5), 918-939.

Zenkour, A.M. (2006), "Generalized shear deformation theory for bending analysis of functionally graded plates", *Appl. Math. Model.*, **30**(1), 67-84.

Zidi, M., Tounsi, A., Houari, M.S.A., Adda Bedia, E.A. and Anwar Bég, O. (2014), "Bending analysis of FGM plates under hygro-thermo-mechanical loading using a four variable refined plate theory", *Aerosp. Sci. Tech.*, **34**, 24-34.

*CC*